

# Fuzzy Visual Servoing for Micro Aerial Vehicles

Andreas Wendel, Michael Maurer, Mario Katusic, and Horst Bischof

{wendel,maurer,katusic,bischof}@icg.tugraz.at  
Institute for Computer Graphics and Vision  
Graz University of Technology, Austria

**Abstract.** We present a visual servoing approach for controlling a micro aerial vehicle which is based on monocular camera input and a fuzzy logic controller. Visual pose estimates are obtained using a state-of-the-art visual SLAM approach combined with marker-based metrical initialization. In comparison to related work, we demonstrate that our system tolerates quickly changing velocity measurements which are commonly observed in visual pose estimation, and that it is well suited for autonomous inspection tasks because it does not require a nadir view onto the scene.

**Keywords:** Visual servoing, micro aerial vehicle, fuzzy logic, non-nadir camera, parallel tracking and mapping, MAV, PTAM

## 1 Introduction

Airborne image acquisition has a long tradition in photogrammetry, surveillance, and inspection. Recent achievements in aerial robotics led to the development of robust and easily usable micro aerial vehicles (MAVs) such as quad-rotor helicopters, which are typically remote controlled but become increasingly autonomous. As an effect, robotic applications emerge in typical human-operated service tasks such as monitoring of oil and gas pipelines, power lines [1], power pylons or large crowds [2]. All applications of autonomous flight require sophisticated mechanisms for automatic take-off, hovering and landing, since these are the critical flight phases.

A variety of algorithms for perception and control of autonomous aerial vehicles has been proposed, mainly because the most suitable technique highly depends on the available sensors. The most common approach is to obtain pose information based on external systems; the Global Positioning System (GPS) is frequently used for outdoor scenes [3], and the Vicon tracking system for indoor scenes [4]. Often, Inertial Measurement Unit (IMU) readings are fused to the external measurement for stabilization and control of the MAV. However, for applications in an outdoor environment such as the inspection of power pylons the accuracy delivered by GPS is not sufficient, and high-precision systems such as differential GPS are not feasible due to cost, weight, and handling issues.

Other approaches rely on sensors which move along with the vehicle and need Simultaneous Localization and Mapping (SLAM) procedures. Autonomous vehicles often incorporate Laser Range Finders (LRFs) to perceive depth directly [5].

However, in outdoor environments LRFs have a restricted perception distance and either the time for scanning an entire volume is considerably high, or the scanner is too heavy for an MAV. In comparison, visual sensors are light-weight, deliver the richest representation of a scene, and can be used for indoor as well as for outdoor applications. Related work in visual localization [6] has shown that a single sensor is enough to estimate motion in 6 degrees of freedom (DoF), and yields higher precision than low-cost GPS sensors. The only drawback is that visual input requires the most computational power to process the data.

In this work, we present a system which provides robust visual servoing for MAVs based on monocular camera input and a fuzzy logic controller. The system is well suited for inspection tasks, because the camera’s pitch angle can be arbitrarily defined and is not restricted to nadir views. The incorporation of a fuzzy controller allows to quickly change payloads as no model knowledge about the MAV is required, and it tolerates quickly changing velocity measurements which are commonly observed in visual pose estimation.

## 2 Fuzzy Visual Servoing

Visual servoing techniques use visual input to control the motion of a robot. In general, the goal is to minimize the error between a desired system state and the noisy measured system state by controlling the system’s variables. For MAVs such as quad-rotor helicopters, it is feasible to control the speed of four rotors independently, or on a higher level to control the three system angles roll  $\Phi$ , pitch  $\Theta$ , and yaw  $\Psi$ , as well as the thrust  $T$ . Given a 6 DoF visual pose estimate, it is also possible to control the position of the MAV in space using Position-Based Visual Servoing (PBVS). A position controller has four inputs, namely the desired position  $(x^*, y^*, z^*)$  and the desired yaw angle  $\Psi^*$ . Roll  $\Phi$  and pitch  $\Theta$  depend on the position commands, as the MAV has to pitch or roll to obtain a certain position. By changing the desired values accordingly, the position controller is used to control an autonomous MAV during take-off, hovering, and landing; in other words, the desired trajectory control for inspection applications is implemented.

The following sections give an overview of our fuzzy visual servoing approach and discuss the advantages with respect to related work. Subsequently, our approach to autonomous take-off and landing is introduced.

### 2.1 System Design and Overview

Our system design incorporates several properties of the flight hardware, the visual perception methodology, and the application of airborne inspection. An overview can be found in Fig. 1.

Many commercially available MAVs, such as the Ascending Technologies Pelican used in this work, already come with an attitude controller which translates angular and thrust commands into rotational speeds [7]. Attitude control is based on IMU and accelerometer readings and provides a good basis for robust and

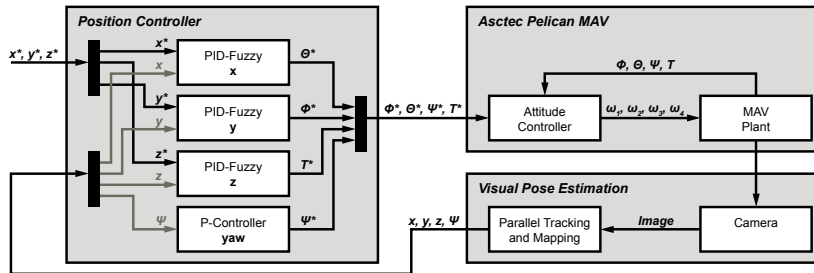


**Fig. 1.** Fuzzy visual servoing. Our system consists of a cascaded control loop with an attitude controller and a position controller. Feedback is received using a camera mounted on the MAV and subsequent processing by PTAM [8]. The position controller consists of three independent PID fuzzy logic controllers and a simple proportional controller to maintain the orientation of the MAV.

stable flight. However, due to the lack of exteroceptive sensors it is prone to drift and bias, and depends on the accuracy of the system model.

Visual pose estimation overcomes this issue. We use a single monocular camera and an adaption of the well-known Parallel Tracking and Mapping (PTAM) [8] algorithm to localize the MAV. PTAM is capable of estimating the current camera pose up to scale by simultaneously tracking image patches and maintaining a bundle-adjusted map. Since visual navigation of an MAV also requires the correct scale, we place a known ARToolKitPlus marker [9] into the scene during initialization. We thus recover a metrical baseline, which leads to correct metrical scaling of the entire map.

In a local environment, PTAM typically delivers good pose estimates within a range of a few centimeters, depending on the distance to the scene. However, the position estimate can considerably jump within that range because of the error propagation of quantized feature measurements. This has a major effect on control: The derivative of the position, i.e. the estimated velocity, suffers from heavy salt-and-paper noise.

Different approaches have been presented to resolve this issue with visual pose input. Kemp [10] maintains a set of multiple smooth position and velocity estimates, where the best is selected based on likelihood and processed using simple PID control. This is similar to particle filtering and thus requires a lot of additional processing power. Bloesch et al. [11] and Achtelik et al. [12] try to accurately model the system in a Linear Quadratic Gaussian control design with Loop Transfer Recovery (LQG/LTR). They incorporate additional sensor information from IMU, accelerometers, and an air pressure sensor to cope with pose estimation uncertainties. While this fusion is beneficial, it requires considerable system knowledge about the aerial vehicle and restricts the flexibility. In contrast, our fuzzy control approach allows to interactively change payloads based on the application, but also to change the set of rules based on the current scene and the corresponding visual pose estimation quality.

**Table 1.** Fuzzy logic rule-set for determining the output based on the current position error  $e_x$  and velocity error  $\Delta e_x$ .

$\Delta e_x \backslash e_x$	<i>BIG_NEG</i>	<i>NEG</i>	<i>CENTER</i>	<i>POS</i>	<i>BIG_POS</i>
<i>NEG</i>	<i>BIG_POS</i>	<i>POS</i>	<i>POS</i>	<i>CENTER</i>	<i>CENTER</i>
<i>CENTER</i>	<i>POS</i>	<i>POS</i>	<i>CENTER</i>	<i>NEG</i>	<i>NEG</i>
<i>POS</i>	<i>CENTER</i>	<i>CENTER</i>	<i>NEG</i>	<i>NEG</i>	<i>BIG_NEG</i>

Finally, airborne inspection tasks require a camera which looks at the scene rather than on the ground. It has recently been shown that this can be achieved with a single camera by interleaving detailed and overview images in a stream [13]. In contrast to most existing approaches [11][12], we do not require a nadir camera view; we do not even require a rigid transformation between the camera and the MAV due to the cascaded controller. Our system only employs the 3D position and the yaw with respect to the scene for control, so mechanical stabilization of the camera is possible and the camera's pitch angle can be arbitrarily defined.

## 2.2 Fuzzy PID Control

The position controller consists of three identical PID fuzzy logic controllers for the individual axes and a proportional controller to maintain the orientation of the MAV. In the following, the controller for the  $x$  axis is described.

Based on the desired position  $x^*$  and the current position  $x$ , the error  $e_x$  and the error change  $\Delta e_x$  can be calculated. Thus, two variables serve as controller input, whereas the output is the desired pitch angle  $\Theta^*$ . The error change

$$\Delta e_x[n] = e_x[n] - e_x[n-1], \quad (1)$$

where  $n$  is the current time, gives a rough estimate for the velocity error. The desired pitch angle  $\Theta^*$  is obtained by integrating the relative change of the pitch angle over time, i.e.

$$\Theta[n]^* = \Theta[n-1]^* + \Delta\Theta[n]. \quad (2)$$

The integration part is necessary to compensate MAV drifts along the roll angle. Moreover, the temporal integration of the fuzzy logic output enables to cope with external influences such as wind, battery drain or turbulences.

A typical fuzzy logic controller consists of three blocks, namely fuzzification, inference and defuzzification. First, the two inputs and the output have to be fuzzified, meaning that the measured values are mapped to the truth values of the fuzzy set. Then, the rule-set of the inference block as shown in Table 1 is applied; it is defined in a way a human expert would control the pitch  $\Theta$  when manually flying the MAV. It can be read in a linguistic way as

$$\mathbf{IF} \ e_x \text{ is } \mathit{BIG\_NEG} \ \mathbf{AND} \ \Delta e_x \text{ is } \mathit{NEG} \ \mathbf{THEN} \ \Delta\Theta \text{ is } \mathit{BIG\_POS},$$

in other words if the position error is large and negative, and the velocity error is also negative then the desired output is large and positive. Based on the five

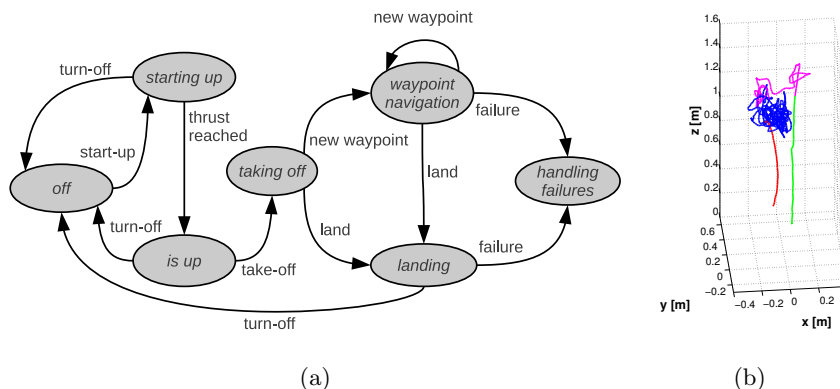


**Fig. 2.** (a) State machine for autonomous flight. (b) MAV trajectory during take-off (green), drift compensation (magenta), hovering (blue) and landing (red).

membership functions of the first input  $e_x$  and three of the second input  $\Delta e_x$ , fifteen rules exist to control the  $x$ -position of the MAV.

Finally, the last block of the fuzzy logic control is the defuzzification. The truth values of the output membership functions are mapped to a real value for the system input. In case of the  $x$ -position controller the change of the pitch angle is computed. We use the Center-of-Area method for defuzzification, where the center-of-gravity of the area of the composited output function is mapped to the  $x$ -axis.

### 2.3 Autonomous Take-off, Hovering, and Landing

Visual servoing is especially beneficial when high positioning accuracy is necessary, namely during take-off, landing, and when hovering close to objects. A state machine demonstrating the individual steps and a resulting trajectory is shown in Fig. 2.

For autonomous take-off, we first acquire a sparse map of the area around the starting point by manually translating the vehicle while looking towards the marker. As the marker can be tilted, the reference coordinate system for navigation is set with an  $xy$ -plane parallel to the ground, based on the IMU readings of the MAV. Finally, the first waypoint is set just above the starting point, and the MAV increases the thrust until it starts climbing and receives the first valid pose estimate. Typically, the missing accurate system model leads to a drift compensation phase where the correct parameters are automatically estimated. Afterwards, the MAV automatically hovers at the commanded waypoint until it receives a new desired position. For landing, we decrease the thrust of the MAV so that a visually supervised decline is initiated. Once the map is lost close to the ground, the MAV continues to decline with the same thrust until it touches the ground.

**Table 2.** Performance for outdoor hovering. The RMS and maximum error for the  $z$  and  $xy$ -plane and in 3D space ( $xyz$ ) are compared to [12].

Approach	Distance [m]	RMS error [m]			Max error [m]		
		$z$	$xy$	$xyz$	$z$	$xy$	$xyz$
Ours, $320 \times 256$ px	10.0	0.0643	0.1495	0.1627	0.2189	0.2716	0.3471
Achtelik et al.[12]	3.3	0.11	0.44	–	–	–	–

### 3 Experiments and Results

We performed several experiments to evaluate the accuracy of our visual control approach which are discussed in the following. To obtain these results, we used an Ascending Technologies Pelican quad-rotor helicopter equipped with a mechanically stabilized industrial camera. We streamed images with a resolution of  $320 \times 240$  px at 30 Hz via a wireless 802.11n link to the ground station. To ensure a reliable connection for control commands, we send control commands over a separate X-Bee wireless data link directly to the MAV’s autopilot.

Note that a fair comparison of our visual servoing approach to other work would only be possible in a simulated environment. All results depend on the scene, the distance to the scene and for outdoor experiments on the wind conditions.

#### 3.1 Hovering Results

For measuring the hovering accuracy in an outdoor setting we hovered directly above the take-off position at an altitude of  $1.5\text{ m}$  and a horizontal mean distance to the feature points in the map of about  $10\text{ m}$ . As error measurement we use the Root Mean Square error (RMS) in individual directions, and we compare our results to the work of Achtelik et al. [12] in Table 2. It can be seen that we are outperforming their approach, although we do not yet incorporate IMU measurements and employ a non-nadir view with larger distance to the scene. An example for the hovering trajectory is visualized in Fig. 2.

#### 3.2 Trajectory Flight Results

Not only the accuracy at a fixed position is important, but also the trajectory between defined waypoints is of interest. Therefore, we evaluated the accuracy of flight trajectories during an indoor experiment. We defined a  $2 \times 2\text{ m}$  square trajectory sampled in path lengths of  $1.0\text{ m}$  at an altitude of  $1.5\text{ m}$  as depicted in Fig. 3 and measured the RMS error in individual directions. The results are compared to those of Bloesch et al. [11] in Table 3. Our results can compete, and we are not dependent on a wired connection between MAV and ground station. Furthermore, we do not rely on a textured ground plane which is often not available when flying above a road or grass, and our approach does not require a system model of the MAV.

**Table 3.** Performance for the trajectory flight. The RMS and maximum error for  $xyz$  are evaluated by sampling along the trajectory in 0.5 mm steps.

Approach	RMS error [m]			
	$x$	$y$	$z$	$xyz$
Ours, $320 \times 256$ px	0.0704	0.1109	0.0663	0.1471
Blösch et al. [11]	0.0995	0.0748	0.0423	—

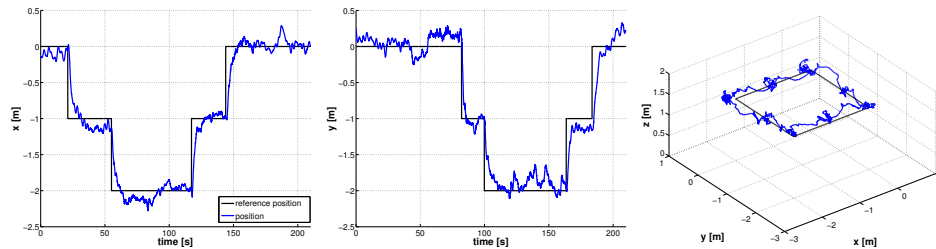


**Fig. 3.** MAV trajectory along a predefined  $2.0 \times 2.0$  m square path. The first two figures show the temporal change of the  $x$  and  $y$  coordinates and the third the spatial representation of the trajectory in 3D space. Waypoints are defined in steps of 1.0 m.

Further results demonstrating our performance during take-off, hovering, and landing, as well as during phases where occlusions of the scene occur, can be found online<sup>1</sup> in form of a video.

## 4 Conclusion

We have presented a robust visual servoing system for MAVs based on monocular camera input and a fuzzy logic controller. The system is well suited for inspection tasks, because the camera’s pitch angle can be arbitrarily defined and is not restricted to nadir views. The incorporation of a fuzzy controller allows to quickly change payloads as no model knowledge about the MAV is required, and it tolerates quickly changing velocity measurements which are commonly observed in visual pose estimation.

In future work we will focus on running the controller on-board by splitting the tracking and mapping processes according to [14]. Additionally, we would like to investigate the adaptation of the fuzzy rules based on the estimated visual input quality.

## Acknowledgments

This work has been supported by the Austrian Research Promotion Agency (FFG) project FIT-IT Pegasus (825841/10397) and Omicron electronics GmbH.

<sup>1</sup> <http://aerial.icg.tugraz.at>

## References

1. Whitworth, C., Duller, A., Jones, D., Earp, G.: Aerial video inspection of overhead power lines. *Power Engineering Journal* **15**(1) (2001) 25–32
2. Mejias, L., Campoy, P., Saripalli, S., Sukhatme, G.S.: A Visual Servoing Approach for Tracking Features in Urban Areas using an Autonomous Helicopter. In: *Proceedings of International Conference on Robotics and Automation, Orlando, US* (2006) 2503–2508
3. Conway, A.R.: *Autonomous Control of an Unstable Model Helicopter Using Carrier Phase GPS Only*. PhD thesis, Stanford University (1995)
4. Michael, N., Mellinger, D., Lindsey, Q., Kumar, V.: The GRASP Multiple Micro UAV Testbed. *IEEE Robotics and Automation Magazine* **17**(3) (2010) 56–65
5. He, R., Prentice, S., Roy, N.: Planning in Information Space for a Quadrotor Helicopter in a GPS-denied Environment. In: *Proceedings of International Conference on Robotics and Automation, Pasadena, CA* (2008) 1814–1820
6. Wendel, A., Irschara, A., Bischof, H.: Natural landmark-based monocular localization for MAVs. In: *Proceedings of International Conference on Robotics and Automation, Shanghai, CN* (2011)
7. Gurdan, D., Stumpf, J., Achtelik, M., Doth, K.M., Hirzinger, G., Rus, D.: Energy-efficient autonomous four-rotor flying robot controlled at 1 khz. In: *Proceedings of International Conference on Robotics and Automation*. (2007) 361–366
8. Klein, G., Murray, D.: Parallel Tracking and Mapping for Small AR Workspaces. In: *Proceedings 6th IEEE and ACM International Symposium on Mixed and Augmented Reality, Nara, JP* (2007) 225–234
9. Wagner, D., Schmalstieg, D.: ARToolKitPlus for Pose Tracking on Mobile Devices. In: *Proceedings 12th Computer Vision Winter Workshop, St. Lambrecht, AT* (2007) 139–146
10. Kemp, C.: *Visual Control of a Miniature Quad-Rotor Helicopter*. PhD thesis, Churchill College, University of Cambridge (2006)
11. Blösch, M., Weiss, S., Scaramuzza, D., Siegwart, R.: Vision Based MAV Navigation in Unknown and Unstructured Environments. In: *Proceedings of International Conference on Robotics and Automation, Anchorage, Alaska* (2010) 21–28
12. Achtelik, M., Achtelik, M., Weiss, S., Siegwart, R.: Onboard IMU and Monocular Vision Based Control for MAVs in Unknown In- and Outdoor Environments. In: *Proceedings of International Conference on Robotics and Automation, Shanghai, CN* (2011)
13. Maurer, M., Wendel, A., Bischof, H.: Airborne inspection using single-camera interleaved imagery. In: *Proceedings of Computer Vision Winter Workshop, Mala Nadelja, SL* (2012)
14. Wendel, A., Maurer, M., Graber, G., Pock, T., Bischof, H.: Dense Reconstruction On-the-Fly. In: *Proceedings of IEEE Conference on Computer Vision and Pattern Recognition, Providence, US* (2012)